Open Research Online

The Open University's repository of research publications
and other research outputs

Mitigating radiation-induced charge transfer inefficiency in full-frame CCD applications by 'pumping' traps

Conference or Workshop Item

For guidance on citations see FAQs.

Version: Accepted Manuscript

Link(s) to article on publisher's website:
http://dx.doi.org/doi:10.1117/12.926804
http://proceedings.spiedigitallibrary.org/proceeding.aspx?articleid=1363332

oro.open.ac.uk

Mitigating Radiation-Induced Charge Transfer Inefficiency in Full-Frame CCD Applications by 'Pumping' Traps

N. J. Murray*[a], A. D. Holland[a], J. P. D. Gow[a], D. J. Hall[a], J. H. Tutt[a], D. Burt[b], J. Endicott[b]

[a]e2v centre for electronic imaging, The Open University, Milton Keynes, MK7 6AA, UK

[b]e2v technologies plc, 106 Waterhouse Lance, Chelmsford, Essex, CM1 2QU, UK

ABSTRACT

The charge transfer efficiency of a CCD is based on the average level of signal lost per pixel over a number of transfers. This value can be used to directly compare the relative performances of different structures, increases in radiation damage or to quantify improvements in operating parameters. This number does not however give sufficient detail to mitigate for the actual signal loss/deference in either of the transfer directions that may be critical to measuring shapes to high accuracy, such as those required in astronomy applications (e.g. for Gaia's astrometry or the galaxy distortion measurements for Euclid) based in the radiation environment of space.

Pocket-pumping is an established technique for finding the location and activation levels of traps; however, a number of parameters in the process can also be explored to identify the trap species and location to sub-pixel accuracy.

This information can be used in two ways to increase the sensitivity of a camera. Firstly, the clocking process can be optimised for the time constant of the majority of traps in each of the transfer directions, reducing deferred charge during read out. Secondly, a correction algorithm can be developed and employed during the post-processing of individual frames to move most of any deferred signal back into the charge packet it originated from.

Here we present the trap-pumping techniques used to optimise the charge transfer efficiency of p- and n-channel e2v CCD204s and describe the use of trap-pumped images for on-orbit calibration and ground based image correction algorithms.

Keywords: CTE, CTI, CCD, pocket pumping, traps, transfer, p-channel

1. INTRODUCTION

This paper describes recent work undertaken at the e2v centre for electronic imaging in support of the visible imager (VIS) for the ESA Euclid space mission in their Cosmic Vision programme.

The primary objective of Euclid VIS is to provide data for Weak Lensing measurements of distant galaxies over a 5-6 year mission [1]. The instrument will detect more than a billion galaxies with a signal-noise ratio >10 and the statistical precision afforded by such a large sample is a prerequisite to constraining the nature of dark energy and dark matter within the Universe through weak gravitational lensing measurements [2]. Given the precision of such a survey, exceptionally tight requirements are placed on the on the knowledge of the shape of the instrument's PSF and its evolution during the mission due to radiation damage mechanisms within the Charge-Coupled Devices (CCDs).

VIS comprises an array of thirty six CCD273s manufactured by e2v technologies, with a broad red bandpass (550 nm to 900 nm) and arranged in a 6x6 matrix on the front of the focal plane array [2][3][4]. The impact on charge transfer efficiency (CTE) due to proton irradiation on the CCD273 and similar e2v devices (CCD204) has been subject to detailed investigations [5][6] and has concluded that under normal operating conditions, the CCD273 satisfies mission requirements within the tolerances placed on the specification. However any further improvement in CTE could allow a relaxation of constraints placed on other VIS sub-systems or yield additional science beyond those of the baseline mission requirements.

*n.j.murray@open.ac.uk; phone 44 1908 332769; fax 44 1908 655910; www.open.ac.uk/cei

1.1 Charge Transfer Inefficiency in CCDs

Figure 1 demonstrates one of the mechanisms by which an electron can be trapped during charge transfer and released into the following potential well, or charge packet, leading to charge transfer inefficiency (CTI). Each step of the single row transfer is represented by a line in the style of the potential well model, where the well (and pixel) is defined by bias applied to combinations of image electrodes labeled one to four.
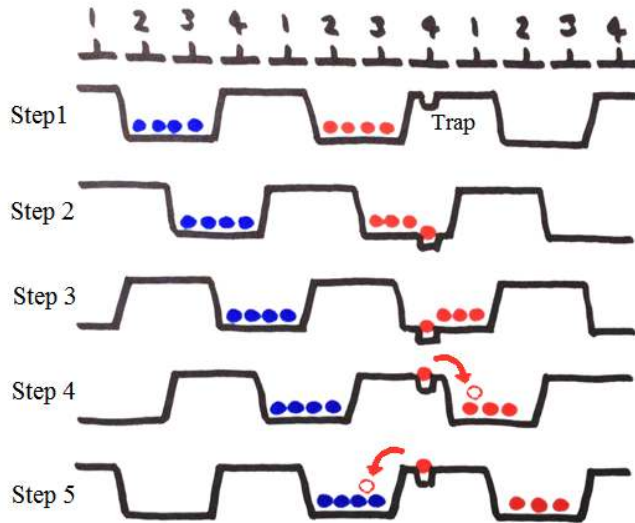

Figure 1. Example of deferred charge caused by a barrier phase trap under an image electrode.

In Step 1 charge is generated and collected in the wells defined by bias applied to image electrodes two and three. Image electrodes one and four are biased to a lower level during this time, typically zero Volts, forming barrier phases in the electrostatic potential along the vertical transfer channel. A single electron trap is represented by the smaller well under image phase four in the central pixel.

In Step 2, the first stage of the transfer, each well structure shifts forward towards the readout register (right) by 1 image electrode. At this point an electron is captured by the trap under electrode four in the central pixel. If the trap releases the electron during Step 3 it will most likely be recaptured immediately and if the electron is released during Step 4 it will have a high probability of re-joining its original charge packet. However if the trap does not release the electron until Step 5, it will have a high probability of being collected in the subsequent charge packet.

1.2 Pocket/trap pumping

Pocket pumping is an established method for locating the presence of charge trapping sites within a CCD array structure [7][8][9]. A flat-field of signal (dark current, photo-generated or electrically injected) is collected and then transferred forwards and backwards by 1 (or more) array elements for a number of cycles. During this time, signal can become trapped from one charge packet during transfer and then later released into another. This results in increased signal in one element and a corresponding reduction of signal from the donor(s). These manifest as the characteristic bright and dark pixel dipoles observed in 'pumped' images and examples are shown in Figure 2.
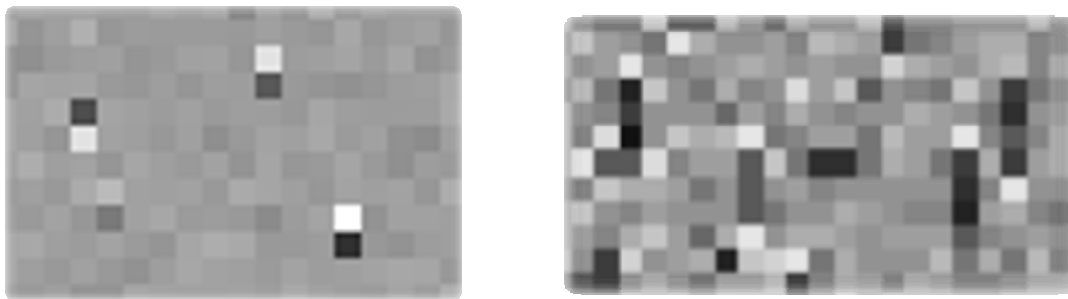

Figure 2. Pumped trap examples for forwards and backwards by 1 image row (left) and 4 image rows (right).

The efficiency of transfer between charge packets is dependent on the number of traps encountered over the transfer range, the location of those traps within the structure (electrode phase and volume) and ultimately the emission time constant of the trap species. This allows the transfer rate, dwell time and operating temperature for 'simple', single-electron per-pixel traps to be explored to provide an understanding of the trap species present.

1.3 Experimental setup

Three types of CCD were used in this work and are summarised in Table 1 and two are shown in Figure 3. Devices were manufactured by e2v technologies and procured by ESA for Euclid VIS pre-development and phase A studies. Inner regions of each device were subject to proton irradiation at room temperature at the expected Euclid end-of-life dose to assess the impacts of space radiation environment at the second Lagrange point (L2) [10]. All devices were cooled by CryoTiger® and nominally stabilised by additional heating to the baseline Euclid VIS operating temperature of 153 K. Both ^{55}Fe and electric X-ray tube sources were used to provide 5,898 eV photons for gain calibration and X-ray CTE measurements. LEDs were used to provide roughly flat field illuminations.

Table 1. Euclid VIS pre-development CCD formats and features

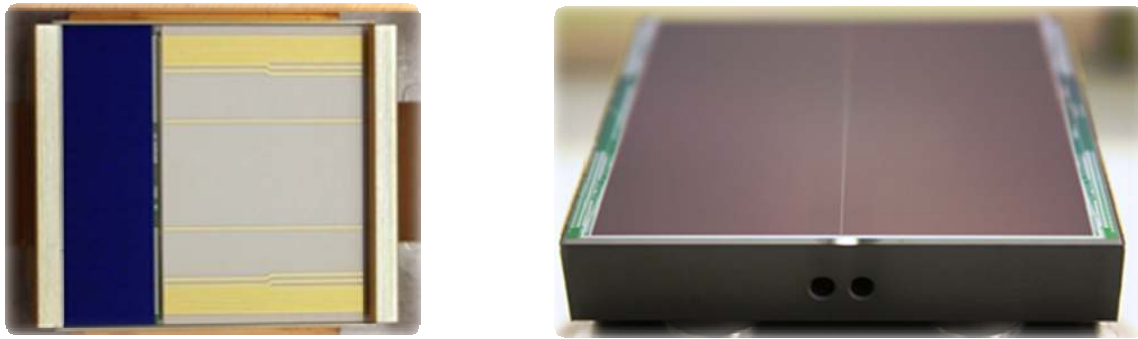|	n-channel CCD204	p-channel CCD204	n-channel CCD273
Architecture	Full-frame	Full-frame	Full-frame
Pixel size	12 μm, square	12 μm, square	12 μm square
Rows	1,064	1,064	4,132
Columns	4,096	4,096	4,096
Image electrodes	4	4	4
Register electrodes	3	3	3
Outputs	2 real, 2 dummy	2 real, 2 dummy	4 real, 4 dummy
Responsivity	4.5 μV/electron	4.5 μV/hole	7 μV/electron
Charge injection	Single gate, upper	Single gate, upper	Two-gate, notched, central
Illumination	Back-face	Back-face	Front-face
Register width	50 μm	50 μm	20 μm

Figure 3. Back illuminated p-channel CCD204 (left) and front-illuminated Euclid VIS CCD273 (right).

2. INCREASED PARALLEL TRANSFER TIMINGS FOR REDUCED CTI

The density of traps observed within a trap-pumped image is a function of the CTE. By 'pumping' under conditions constrained by those of the readout regime it is possible to quickly explore the effects on any free parameter. For Euclid VIS the only free parameter is the transfer rate as the operating temperature is fixed at 153 K and the dwell time is governed by the register read time. The baseline pixel rate for VIS was originally 200 kHz and therefore a dwell time of 10 ms was used in this work. The pixel rate has since been reduced to 70 kHz, moving the dwell time closer to that of the emission time constant of the P-Ci (E~0.30eV) trap species; however this has negligible impact on the data. Traps will be more efficiently pumped and show with greater contrast in the trap pumped image when the transfer rate is similar to the trap's release time constant. The transfer rate is governed by the number of parallel clocking states, each of which have a finite duration commonly referred to as t_{oi} in e2v literature and is typically ~10 μs. Figure 4 shows an example line transfer scheme for a 4-phase device such as the CCD273 (delay times t_{drt} and t_{dtr} are typically equal to t_{oi}).
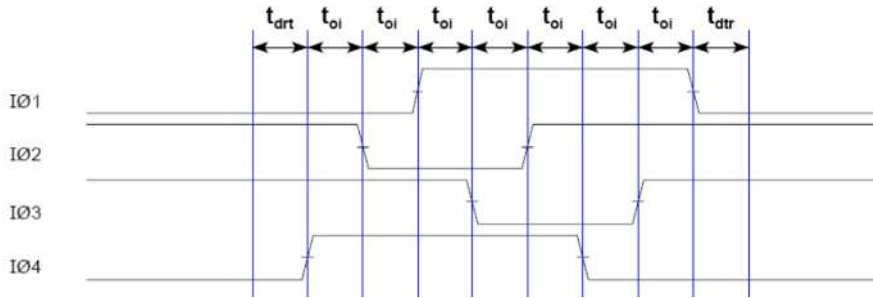
Figure 4. Parallel clocking scheme for standard frame readout [CCD273 ICD].

Parallel clock timings (t_{oi}) were investigated in the region 2 μs to 2,000 μs. Figure 5. highlights the effect on pumped trap density by increasing t_{oi} significantly.
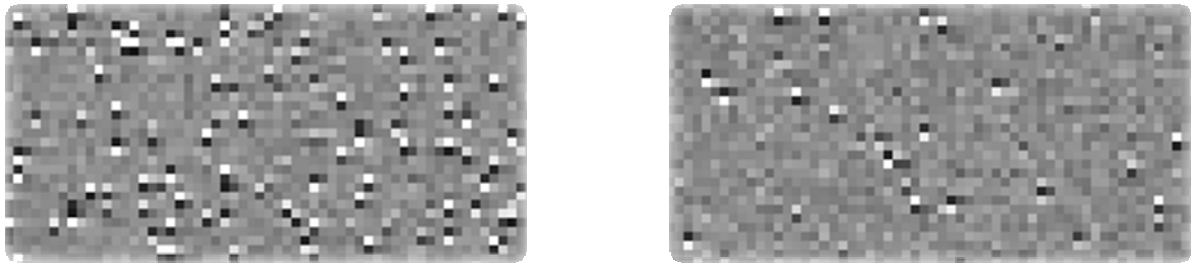

Figure 5. Pumped image sections from proton irradiated CCD204 (4.8E9p.cm-2, 10MeV equivalent). Left: t_{oi} = 10 μs.
Right: t_{oi} = 1,000 μs. Note, images shown are not from the same area of device.

The mechanism by which trap pumping efficiency is being reduced and ultimately CTE increased by elongated parallel transfer clocks is described in the following Figures 6 and 7, accounting for both traps physically located under barrier phase and collecting phases during integration respectively.
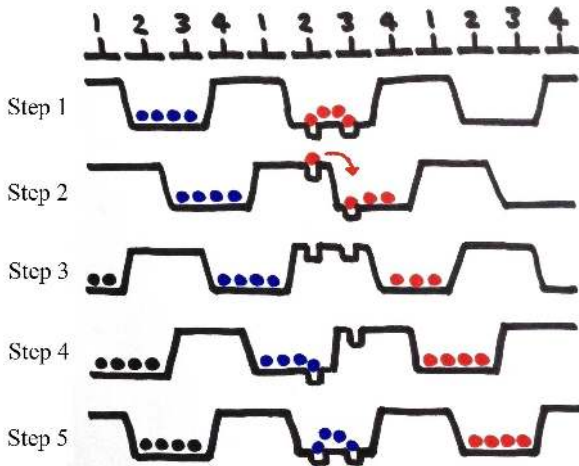

Figure 6. Reducing probability of deferred charge caused by collecting phase traps by increasing t_{oi}.

Figure 6 shows a simplified example for mitigating CTI for traps located under the collecting phase electrodes (two and three), i.e. those biased during integration in Step 1.

In the first stage of charge transfer, the well structure is clocked forward as shown by Step 2, so that the well is now defined by the field created by electrodes three and four and a red electron remains captured somewhere under electrode two. If this condition is then held for a period of time greater than then the emission time constant of the trap species, then the red electron will be released and have a high probability of being attracted back into the well structure that it originated from.

This clocking and waiting sequence then continues for every other step of the complete charge transfer.
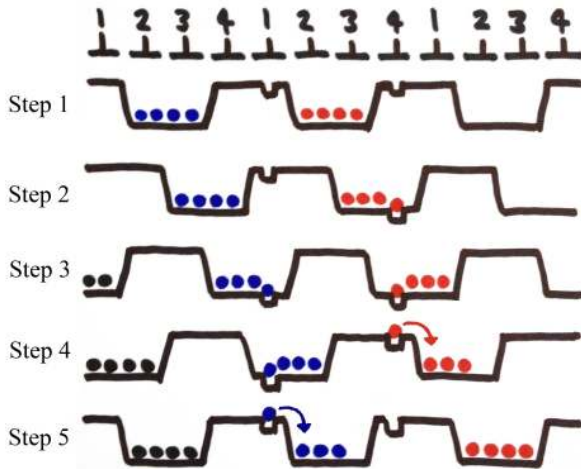
Figure 7. Reducing probability of deferred charge caused by a barrier phase traps by increasing t_{oi}.

Similarly, Figure 7 shows the effect of increased parallel transfer timings for traps located underneath the barrier phase electrodes one and four.

Again charge is collected during integration under electrodes two and three and clocked forward in Step 2. At this point a red electron encounters a trap, becomes trapped and is assumed to remain filled during Steps 2 and 3 regardless of their duration as the capture time may be in the order of nanoseconds.

It is not until Step 4 that the trap holding the red electron can release it without it immediately recapturing. The red electron now has a high probability of being attracted back into its original charge packet (or well structure).

Note that in these examples a coincident clocking scheme is shown whereby there are no overlaps and charge is moved from wells defined by two electrodes directly into the next pair. However, the standard clocking scheme shown in Figure 4 has additional steps where the well structures increases to three electrodes wide in between each of the steps shown in Figures 6 and 7. During these additional steps, trapped electrons in the barrier phase may have a higher probability of being released and captured in the subsequent well structure, as the structure is physically closer to the trap site. Charge transfer inefficiency measurements comparing the effect of increased parallel clock timings for both clocking schemes are presented and discussed in Section 3.1.

2.1 Pumping efficiency vs. line transfer

The number of transfers for each pumped image was chosen to be 1,603 times, allowing an equivalent signal to an [55]Fe photon sampled for traps pumped at 100% efficiency. Figure 8 (Left) demonstrates numerically the effect of slowing down the parallel transfer that was shown in Figure 5. The number of 'pumped' traps is the integral of the curve to the right of the background distribution. In both the control and proton irradiated Regions Of Interest (ROI), the number is reduced significantly when increasing t_{oi} from 10 μs to 1,000 μs.
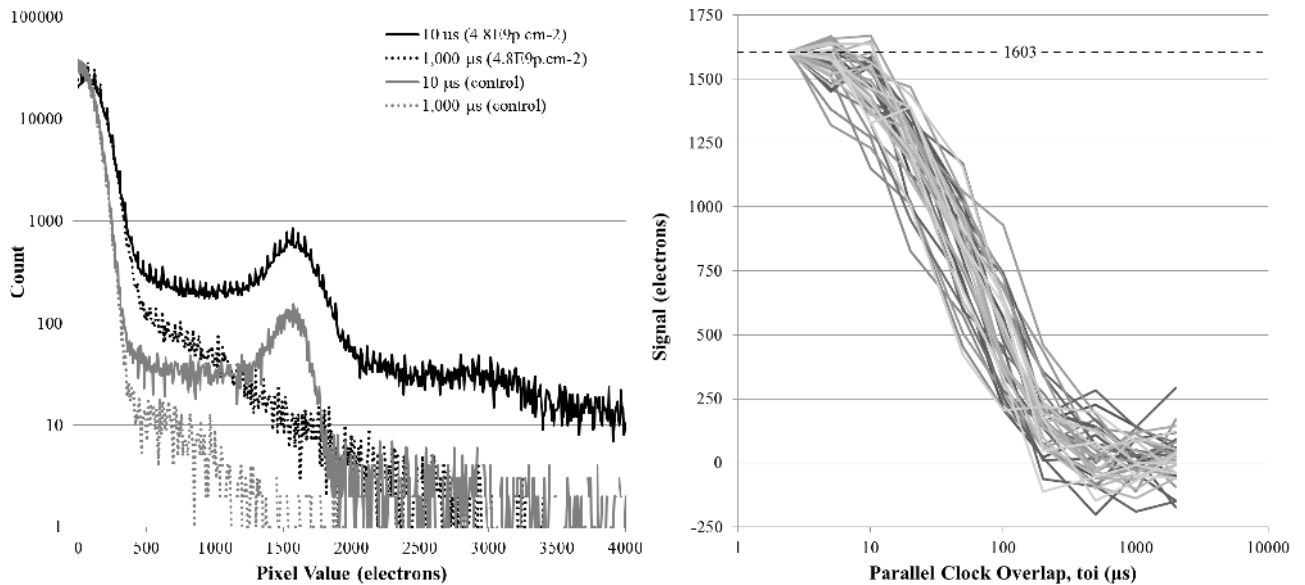

Figure 8. Left: Histograms of pumped signal vs. parallel clock overlap time and proton irradiation. Right: Change in pumping efficiency vs. parallel clock overlap time for 40 example traps efficiently pumped at 2.5 μs.

Figure 8 (Right) shows the effect on forty individual pumped traps of the same species that were most efficiently pumped in the irradiated ROI at t_{oi} = 2.5 µs. When t_{oi} is increased towards the release time constant of this particular trap species the probability of charge releasing and becoming attracted and collected by the potential well is increased and the pumped signal reduces to zero.

2.2 Trap density vs. line time

Figure 9 shows the trap density in the irradiated ROI after proton irradiation to the expected end of life fluence for Euclid that is 4.8E9 p.cm-2 (10 MeV equivalent). This is the number of pixels in the ROI divided by the integral of the curve above a 3-sigma threshold from the background distribution.
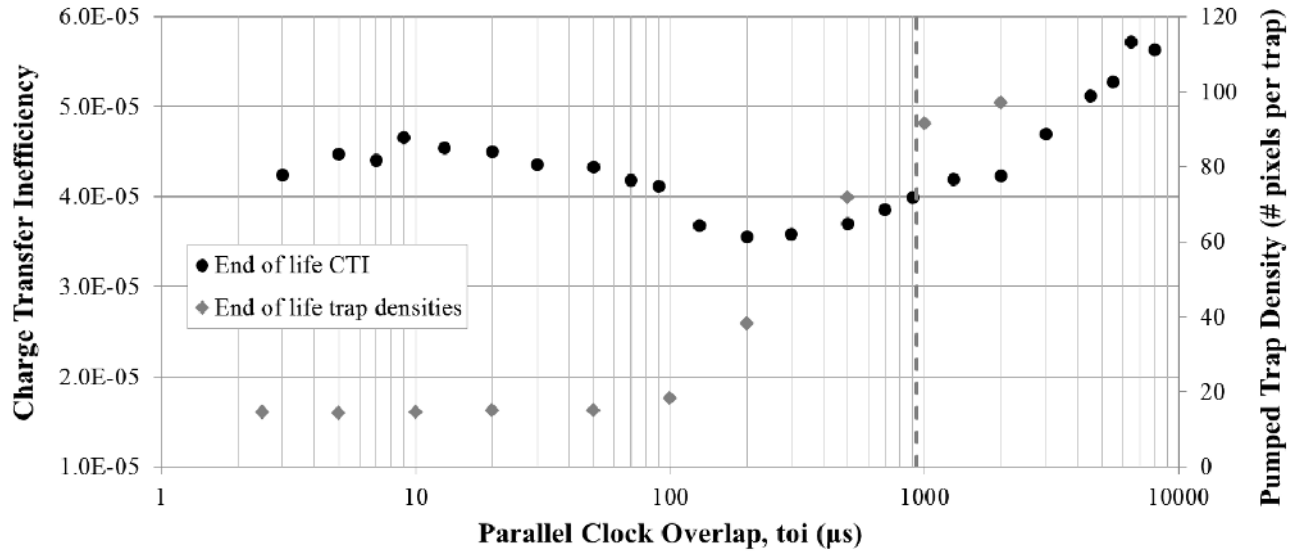

Figure 9. Plot of measured CTI by X-ray and trap density through trap-pumping in region irradiated to 4.8E9 p.cm-2, expected Euclid VIS end of life (EOL). T=153K. The phosphorous divacancy is shown at ~930 µs.

Also plotted in Figure 9 are measurements of CTI taken from the gradient of charge loss in [55]Fe events over the number of parallel transfers using the standard clocking scheme. In both plots we see a change in behaviour for t_{oi} > 100 µs and assume that for these times the majority of trap species have been allowed sufficient time to re-emit any trapped electrons back into their original charge packet or well structure as described by Figures 6 and 7.

It is not currently understood why CTI begins to increase again for t_{oi} > 1,000 µs, but may be due to the single barrier phase during the periods where the well structures are defined by three electrodes or moving into the regime of longer time constant trap species.

It should also be noted that the trap density was calculated from the total number of traps identified from trap pumping, but this in itself only accounts for approximately half the number of traps present in the device as collecting phase traps are not pumped by the scheme described earlier. However this density includes both forward and backwards traps (bright-dark and dark-bright dipoles) as barrier phase traps are pumped in both directions during the process and only dark-bright pairs will give rise to CTI during readout of the device under normal operating conditions.

2.3   Pumping efficiency and CTI vs. operating temperature

In agreement with earlier work at Lawrence Berkeley National Laboratory [9], the temperature dependence of the emission time constant of a trap species (hole or electron) close to that of the transfer rate can also alter the 'pumping' efficiency and ultimately CTI. In Figure 10 we see a significant reduction in the number of traps efficiently pumped at a transfer rate of 10 µs per clocking sequence, when raising the operating temperature by 40 K. This is due to reduced emission time constants for those traps from increased thermal energy and therefore reducing the probability of being efficiently pumped during the fixed timing of the sequence.
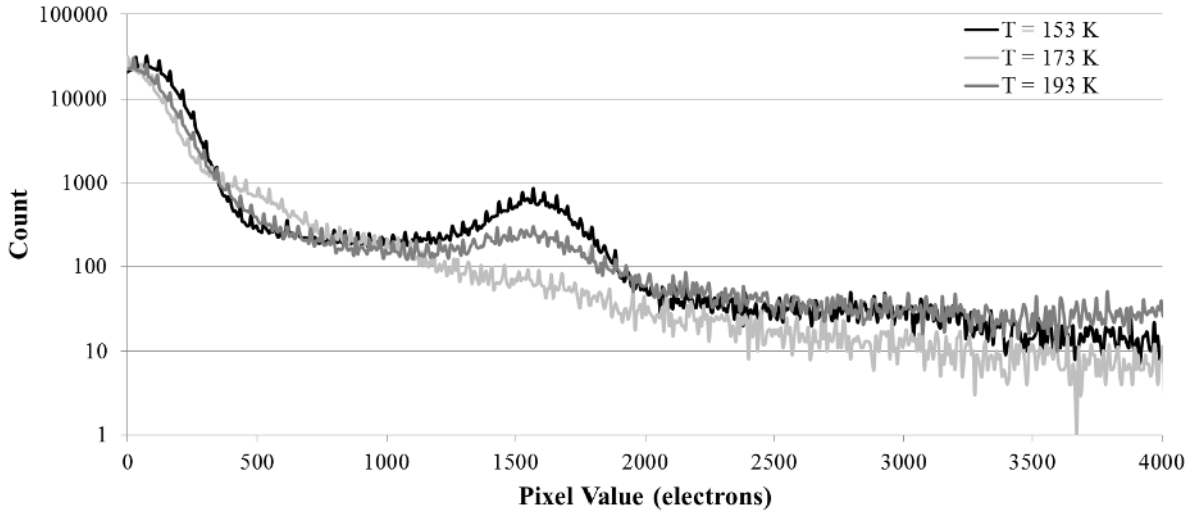
Figure 10. Temperature dependence of pumped signal efficiency in region irradiated to 4.8E9 p.cm-2 (t_{oi} = 10 µs).

By calculating CTI from deferred charge measurements of ^{55}Fe events throughout the irradiated ROI, we see a similar trend in that the improvement gained in CTI arising from increased t_{oi} requires a larger value as the operating temperature is reduced. This is observed as the shift to the right of the trough in the curves in Figure 11.
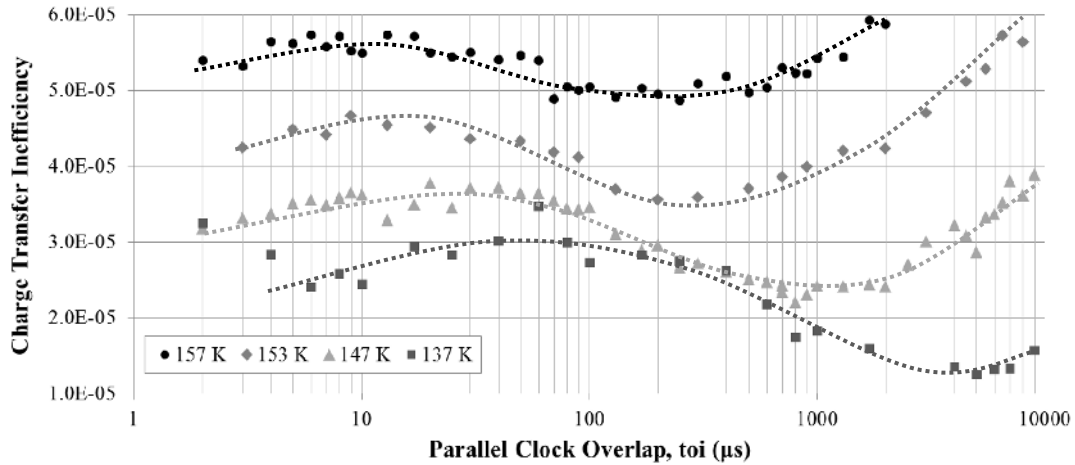

Figure 11. Change in CTI as function of temperature and parallel clock overlap time in region irradiated to 4.8E9 p.cm-2.

3. OPTIMISED PARALLEL TRANSFER CLOCKING SCHEME

3.1 Coincident mode clocking

In Section 2 it was suggested that the standard parallel clocking scheme may not yield the full benefits of increased overlap times, as during the steps where three electrodes are held at high amplitude an electron escaping from a trap in the single barrier phase had an equal probability of finding its original charge packet or the subsequent charge packet or well structure. Both standard and coincident clocking schemes are shown in Figure 12.

X-ray CTI measurements for both schemes are plotted in Figure 13 as a function of the parallel overlap time, t_{oi}. We see a similar trend for both schemes up until 200 µs where the standard scheme begins to increase in CTI, whereas the coincident mode continues to show improvement for significantly longer values of t_{oi}.
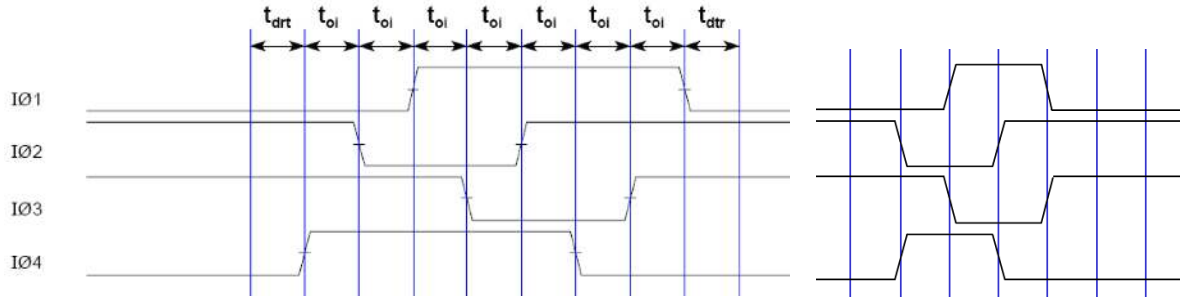
Figure 12. Standard and coincident mode parallel clocking timing diagrams. In both schemes, charge is integrated under two phases, image electrodes IØ2 and IØ3. The first step during charge transfer in the standard scheme initially elongates the well structure by including IØ4, before removing IØ2. In the coincident scheme, the well structure is moves directly from IØ2+IØ3 to IØ3+IØ4.
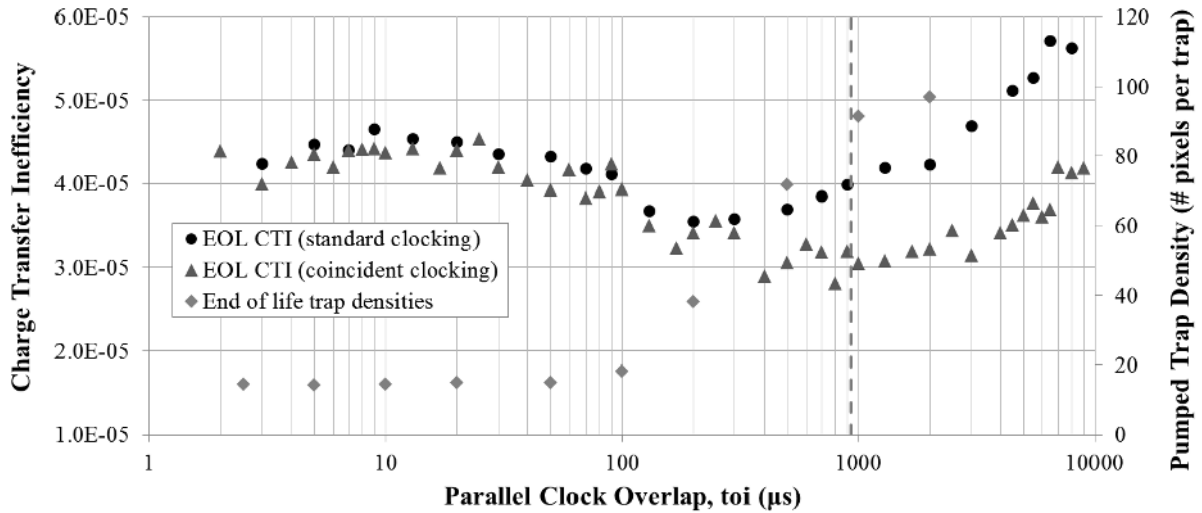

Figure 13. Comparison of measured CTI for standard and coincident clocking schemes in region irradiated to 4.8E9 p.cm-2, expected Euclid VIS end of life (EOL). T=153K. The phosphorous divacancy is shown at ~930 µs.

The trough of the coincident scheme is now at a point where we expect to see it, if we have indeed suppressed the effect of the V-V traps.

4. TRAP PUMPING FOR ON-ORBIT INSTRUMENT CALIBRATION

Provided a suitable flat-field is achievable, a relatively simple trap pumping sequence could be employed on-orbit in some CCD applications, returning very useful data for calibration, ground-based correction algorithms and radiation damage monitoring. In the case of Euclid VIS, sufficient resources are available to provide a single frame of trap-pumped data from each of the thirty six devices on a daily basis, using the fixed level charge injection structure to input flat-fields of between 2,000 to 5,000 electrons. The following sub-sections describe how such data would be particularly beneficial for Euclid VIS.

4.1 Instrument gain calibration

In most CCD applications it is necessary to know what 1 sampled unit returned from the camera is worth in terms of number of electrons. Intrinsic traps present in each of the thirty six devices of VIS can be characterized prior to launch using the on-orbit scheme providing a pumped signal peak similar to that of the 1,603 electrons shown in Figure 8. Providing that the operating temperature and transfer timings are stable to a reasonable accuracy, the behavior of each trap will remain constant until such time that a local on-orbit radiation damage mechanism alters its behavior. Assuming an intrinsic trap density of the order 1 trap in 1,000 pixels, the probability of this occurring remains low long into the mission.

4.2 Post processing data

With knowledge of the location of traps and their relative efficiencies within the CCD array, it may be possible to predict and correct with high accuracy the position of individually deferred electrons, rather than relying on traditional average across-the-array CTI based correction algorithms. This information will be of most use for Euclid VIS and is the subject of on-going study that is discussed in Section 5.

4.3 Radiation damage monitoring

By analyzing frames provided by Euclid VIS on a daily basis, it will be possible to directly measure the radiation damage caused to CCDs at the second Lagrange point (L2) that can then be cross-referenced to the solar activity recorded by other instruments and missions. Such knowledge could then feed back into the models used to predict and optimize the performance of future missions to L2, let alone providing a very interesting time-lapse sequence.

5. CONCLUSIONS

This paper describes some of the techniques developed and modifications to the normal operating modes of the full-frame CCD273/CCD204 for improved charge transfer efficiency. As a consequence of this work, three changes to the standard operating modes are recommended for the Euclid VIS CCDs:

- Increasing the parallel transfer clock timings (t_{oi}) from 10 μs per step to 1,000 μs. This gives a factor ~1.6 improvement in CTE with negligible effect on other systems due to the increased read time.

- Changing the parallel clocking scheme changed to the coincident scheme described in Section 3.1, giving a further 25% reduction in CTI.

- Adopting an equal mode serial clocking scheme without overlapping clock edges.

Given that the necessary resources are available, it would be highly beneficial to both the science of Euclid VIS and future CCD missions at L2 for trap pumping be included as part of the routine calibration images for ground correction algorithms and radiation damage monitoring.

There is a clear relationship between the number of traps observed by trap-pumping and measured CTI. Further study is planned on another CCD273 to be irradiated to fluence approximately one quarter of the expected Euclid end of life dose to investigate number of traps identified vs. signal loss on a column-by-column basis.

REFERENCES

[1] Refregier, A. et al., "Euclid Imaging Consortium Science Book", arXiv:1001.0061, (2010).

[2] Cropper M. *et al.*, "VIS: the visible imager for Euclid", Proc. of SPIE, Vol. 8442 (2012).

[3] Duvet L., "CCD273 Specification", ESA Document SRE-PA/2010.051 (2010).

[4] Endicott J., "Charge-coupled devices for the ESA Euclid M-class Mission", Proc. of SPIE, vol. 8453 (2012).

[5] Gow J. P. D., *et al.*, "Assessment of space proton radiation-induced charge transfer inefficiency in the CCD204 for the Euclid space observatory", Journal of Instrumentation vol. 7, (2012).

[6] Hopkinson G., "CCD 204 preliminary test report", SSTL Document OABE 0139435 (2010).

[7] Janesick J. R., "Scientific Charge Coupled Devices", SPIE Press Washington, (2001).

[8] Kohley, R., "Gaia: operational aspects and tests of Gaia Flight Model CCDs", Proc. of SPIE, Vol. 7439 (2009).

[9] Mostek N. J., *et al.*, "Charge trap identification for proton-irradiated p+ channel CCDs", Proc. of SPIE, Vol. 7742 (2010).

[10] Gow J.P.D., et al., "Effect of decreased register volume on the radiation-induced CTI in the CCD detector for the Euclid VIS Instrument", Proc. of SPIE, Vol. 8453 (2012).